ChemComm

Accepted Manuscript

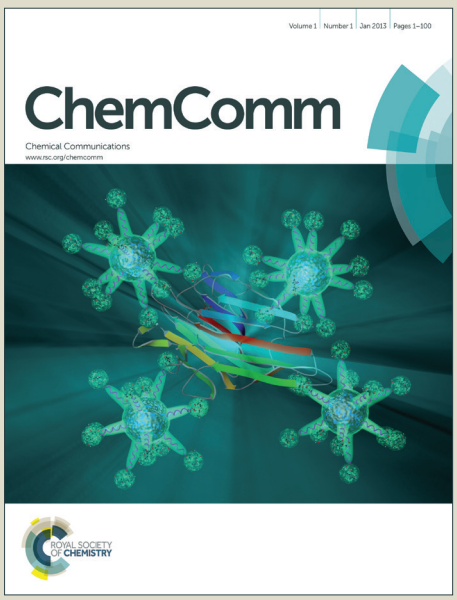

This is an *Accepted Manuscript*, which has been through the Royal Society of Chemistry peer review process and has been accepted for publication.

Accepted Manuscripts are published online shortly after acceptance, before technical editing, formatting and proof reading. Using this free service, authors can make their results available to the community, in citable form, before we publish the edited article. We will replace this *Accepted Manuscript* with the edited and formatted *Advance Article* as soon as it is available.

You can find more information about *Accepted Manuscripts* in the Information for Authors.

Please note that technical editing may introduce minor changes to the text and/or graphics, which may alter content. The journal's standard Terms & Conditions and the Ethical guidelines still apply. In no event shall the Royal Society of Chemistry be held responsible for any errors or omissions in this *Accepted Manuscript* or any consequences arising from the use of any information it contains.

ROYAL SOCIETY OF CHEMISTRY

www.rsc.org/chemcomm

Please do not adjust margins

Journal Name

COMMUNICATION

General strategy for fabricating flexible magnetic silica nanofibrous membranes with multifunctionality

Yang Si,[abc] Chengcheng Yan,[ab] Feifei Hong,[a] Jianyong Yu[c] and Bin Ding[abc*]

Received 00th January 20xx,
Accepted 00th January 20xx

DOI: 10.1039/x0xx00000x

www.rsc.org/

Flexible, magnetic, and hierarchical porous $NiFe_2O_4$@SiO_2 nanofibrous membranes were prepared by combining gelatin method with electrospun nanofibers. The membranes exhibited prominent mechanical strength and mesoporosity, as well as multifunctionality of magnetic responsiveness, dyes adsorption, and emulsion separation.

Silica nanofibrous membranes (SNF) are of great interest in the fields ranging from electronic devices and bioengineering to environmental remediation.[1-3] Particularly, introducing magnetic property into SNF is a critical challenge for next generation of multifunctional membranes that were applied to drug delivery, medical diagnosis, ferrofluids, separation, magnetic resonance imaging, and magnetic adsorption.[4,5] A number of methods, such as hydro-thermal synthesis, self-gelation, and chemical vapour deposition have recently been developed to fabricate magnetic SNF.[6-8] However, as with most of the existing porous silica materials, the resulting SNFs are generally brittle and have small recoverable deformation before failure unless they are infiltrated with an elastomeric polymer.[9,10] Therefore, providing both magnetic property and flexibility to SNF would unlock the significant technological perspectives. Alternatively, electrospun nanofibers, which are at the forefront of advanced fibrous materials, combine the robust mechanical strength, fine flexibility, low density, extremely high aspect ratio, and ease of scalable synthesis from various materials (polymer, ceramic, metal, carbon, and so on).[11-13] These fibers hold great promise as an exceptional precursor for constructing mechanical robust SNF for widespread applications. Herein, we present a general strategy to create magnetic $NiFe_2O_4$@SiO_2 nanofibrous membranes ($NiFe_2O_4$@SNF) with a hierarchical porous structure and flexibility by combining gelatin method with electrospun nanofibers. The electrospun silica nanofiber networks were used as templates for the non-agglomerated growth of 20-50 nm $NiFe_2O_4$ nanoparticles ($NiFe_2O_4$ NPs), thereby forming hierarchical ferromagnetic membranes. The premise for our design is that, unlike liquid-swollen gels and ferrogels, these magnetic membranes are flexible, lightweight, mesoporous, and can be actuated by a small magnet. With their flexibility, selective wettability, high porosity, and large surface area, these membranes exhibited multifunctionality in terms of excellent magnetic responsiveness, efficient adsorption for organic dyes, and effective separation of oil/water emulsions.

We designed the $NiFe_2O_4$@SNF based on two criteria: (1) the silica nanofibers must assemble into a flexible interlaced network, (2) the $NiFe_2O_4$ NPs must be non-agglomerated and firmly incorporated with silica nanofibers at high content. The first requirement was satisfied by the sol-gel electrospinning method. To satisfy the second criterion—the non-agglomerated growth of $NiFe_2O_4$ NPs—we used a versatile and readily accessible gelatin dip-coating method. Fig. 1a describes the synthesis pathway. The electrospun SNF was first fabricated by calcination of tetraethyl orthosilicate/poly(vinyl alcohol) composite gel nanofibers which were generated from a silica sol as described in ESI. Following this, the SNF was dipped in a mixed aqueous solution containing $FeCl_3$ and $NiCl_2$ (a mole ratio corresponding to the nominal composition of Fe:Ni ratio of 2:1) and gelatin (2 wt%). Subsequently, the SNF was dried in an oven, and placed in a microwave oven with power of 400 W for 3 min, leading to the formation of the crosslinked gelatin layer on fiber surface which contained embedded metal salts (gelatin/SNF).[14] Finally, the obtained gelatin/SNF was calcined at 750°C in N_2 flow to generate the brown magnetic $NiFe_2O_4$@SNF, as demonstrated in Fig. 1b. Due to the simplicity of the assembly process in our methodology and the facile availability of electrospun nanofibers, the synthesis can be completed within a day, even on a large scale.

[a] Key Laboratory of Textile Science & Technology, Ministry of Education, College of Textiles, Donghua University, Shanghai 201620, China.
[b] State Key Laboratory for Modification of Chemical Fibers and Polymer Materials, College of Materials Science and Engineering, Donghua University, Shanghai 201620, China.
[c] Nanomaterials Research Center, Modern Textile Institute, Donghua University, Shanghai 200051, China.
Electronic Supplementary Information (ESI) available: [FE-SEM image, mechanical test results, emulsion properties, Movie S1 and S2]. See DOI: 10.1039/x0xx00000x

ChemComm Accepted Manuscript

Please do not adjust margins

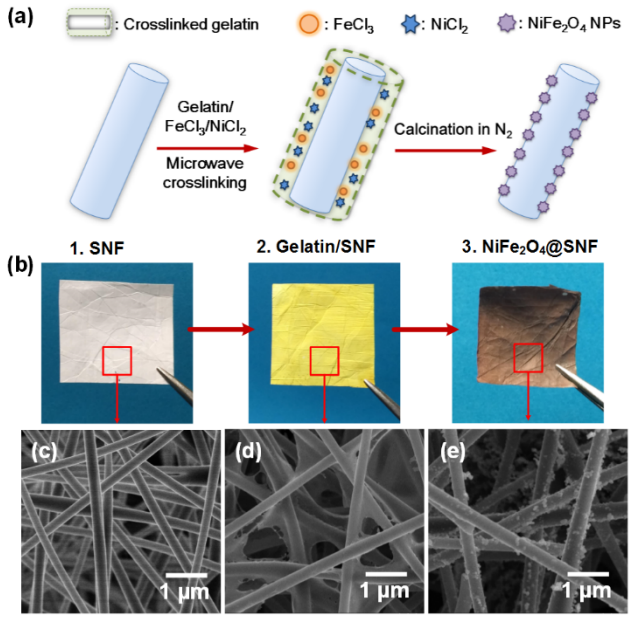

Fig. 1 (a) Schematic showing the synthetic steps of the $NiFe_2O_4$@SNF. (b) Photographs of the SNF, gelatin/SNF, and $NiFe_2O_4$@SNF. Field emission scanning electron microscopy (FE-SEM) images of (c) SNF, (d) gelatin/SNF, and (e) $NiFe_2O_4$@SNF.

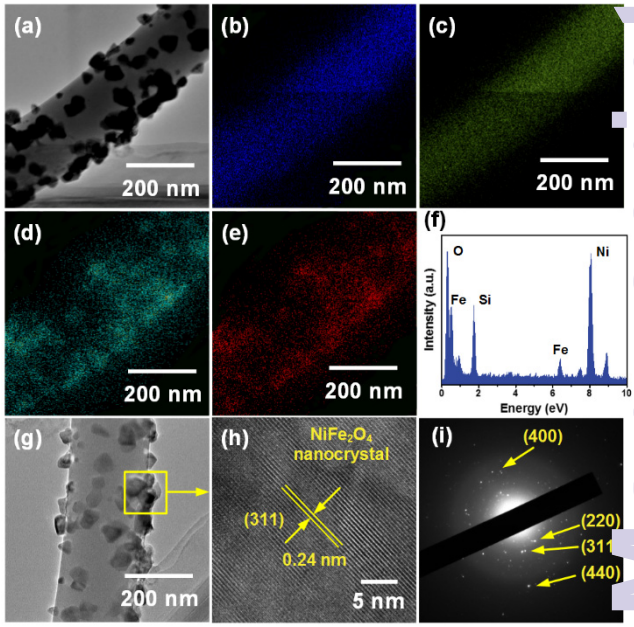

Fig. 2 (a-e) STEM images of the $NiFe_2O_4$@SNF with corresponding elemental mapping images of (b) O, (c) Si, (d) Fe, and (e) Ni, respectively, on a single fiber. (f) EDX spec of $NiFe_2O_4$@SNF. (g) TEM and (h) HRTEM showing the $NiFe_2O_4$ nanocrystals in (311) orientation. (i) SAED pattern of $NiFe_2O_4$@SNF.

As shown in Fig. 1c, the pristine SNF exhibited an obvious 3D open-cell nonwoven geometry with an average fiber diameter of 215 nm, and these fibers were highly interlaced with each other. Upon gelatin treatment, obvious adhesion and increase in fiber diameter (248 nm) could be observed in gelatin/SNF (Fig. 1d), demonstrating the accomplishment of gelatin layer on fiber surface. Evidence for the formation of crosslinked gelatin layer also came from FT-IR spectral analysis (Fig. 3a and ESI).[15] Of particular interest is that the gelatin processes the ability to associate with metal ions through the amino and carboxylic groups;[16,17] thus, it simultaneously loaded lots of iron and nickel ions in its structure during dip-coating process, which acted as an effective carrier and fixative for metal ions. After the following calcination, the gelatin was gradually decomposed, meanwhile, the loaded iron and nickel ions in gelatin layer converted to magnetic $NiFe_2O_4$ NPs via in-situ growth.[18,19] Micrographs of $NiFe_2O_4$@SNF exhibited that the $NiFe_2O_4$ NPs were well located on the fiber surface with a uniform diameter range from 20-50 nm (Figs. 1e and S1).

The scanning transmission electron microscopy (STEM) and energy-dispersive X-ray (EDX) mappings were used to further verify the structure composition of $NiFe_2O_4$@SNF. Figs. 2a-e proved that the Fe and Ni elements were homogeneously distributed throughout the silica fibers at the nanoscale. Based on the semi-quantitative estimation of EDX (Fig. 2f), the calculated content of $NiFe_2O_4$ NPs in membranes was 31.6 wt%, demonstrating that the SNF with high magnetic nanoparticle content could be achieved in the easy, general, and scalable process. Moreover, during the preparation of the STEM specimen, $NiFe_2O_4$ NPs were still incorporated on the surface of fibers after a long-time sonication (15 min), implying the strong interaction between $NiFe_2O_4$ NPs and fibers. This could be attributed to the bonding effect by the residual carbon derived from the incomplete decomposition of gelatin.[6,16] The TEM image presented in Fig. 2g showed that the $NiFe_2O_4$ NPs we partially inlayed in the silica fiber surface. Careful examinatio of high-resolution TEM (HRTEM) image (Fig. 2h) revealed th well-resolved lattice fringes with an interplane distance of 0.2 nm coming from the (311) plane of $NiFe_2O_4$.[16,18] Th corresponding selected-area electron diffraction (SAED) and X ray diffraction (XRD) patterns (Fig. 2i and 3b) revealed th crystalline spinel structure of $NiFe_2O_4$ NPs, which are consisten with the standard XRD data for the $NiFe_2O_4$ phase (JPPDS N 10-0325, see details in ESI).[18,20] The crystallite sizes of $NiFe_2O_4$ NPs determined by Scherrer equation were in the range f n 20 to 40 nm, which matched well with the above FE-SEM observation.

The unique feature of $NiFe_2O_4$@SNF is that the introductio of $NiFe_2O_4$ NPs created the pristine SNF with hierarchical poro structure, thus significantly increasing the porosity and effectiv surface area. As demonstrated in Fig. 3c, the relevant isotherm exhibited the isotherm of type IV with a series of typica adsorption behaviours, revealing characteristics of mesopore within as-prepared membranes.[19] In the case of $NiFe_2O_4$@SNF sample, an obvious H1 hysteresis loop in the P/P_0 region of 0. 0.9 could be observed, revealing that the mesopores are open.[5,21] Significantly, the calculated Brunauer- Emmett-Te er (BET) surface area of SNF, gelatin/SNF, and $NiFe_2O_4$@SNF w re 6.26, 5.07, 42.87 m^2 g^{-1}, respectively, indicating the major contributing role of $NiFe_2O_4$ NPs on deciding the surface area In addition, the Barrett-Joyner-Halenda (BJH) porous structu e analysis revealed that $NiFe_2O_4$@SNF exhibited a typical mesoporous feature with an average pore width of 7.88 nm an a high pore volume of 0.086 cm^3 g^{-1}.

ChemComm Accepted Manuscript

This journal is © The Royal Society of Chemistry 20xx

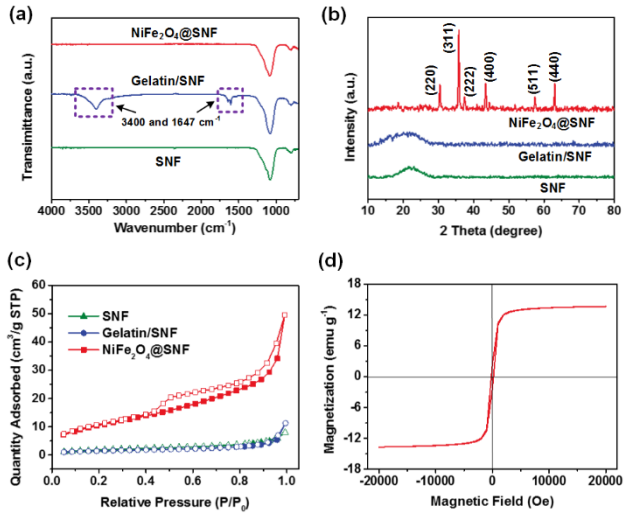

Fig. 3 (a) FT-IR spectra of SNF, gelatin/SNF, and $NiFe_2O_4$@SNF. (b) XRD patterns of SNF, gelatin/SNF, and $NiFe_2O_4$@SNF. (c) N_2 adsorption-desorption isotherms of SNF, gelatin/SNF, and $NiFe_2O_4$@SNF. (d) Magnetic hysteresis loop of $NiFe_2O_4$@SNF measured at 300 K.

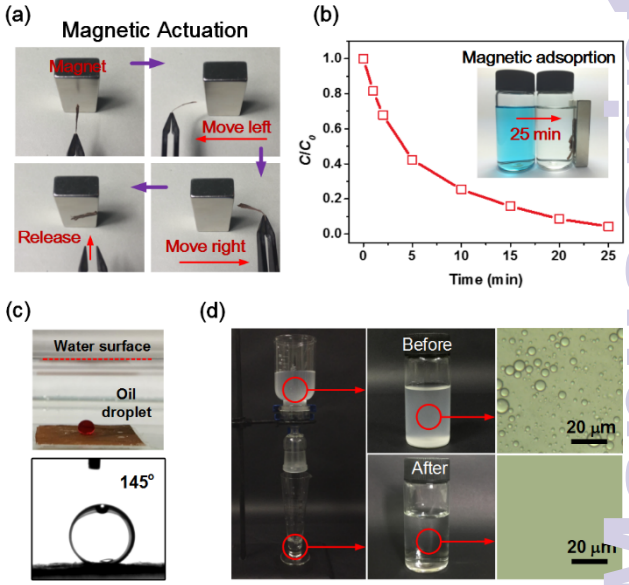

Fig. 4 (a) A piece of $NiFe_2O_4$@SNF is held using tweezers upon a magnet, then the membrane bended towards the magnet when the tweezers move left or right, and it immediately flied to the magnet after being released. (b) The C/C_0 versus time plots for adsorption of dye solution, the inset shows the magnetic responsive of $NiFe_2O_4$@SNF after adsorption of MB for 25min. (c) Photograph of an underwater oil droplet (dyed red) and the measurement of underwater OCA on $NiFe_2O_4$@SNF. (d) Separation apparatus with the facile gravity-driven separation of oil/water emulsions using the $NiFe_2O_4$@SNF and the microscopic images of emulsions before and after separation.

The *M-H* curve displayed in Fig. 3d showed a nonlinear and reversible behavior with a very weak magnetic hysteresis loop. This curve was typical for a soft magnetic material and indicated hysteresis ferromagnetism in the field range of ±1000 Oe,[18] while outside this range the specific magnetization increased with increasing field and saturated in the field range investigated. Moreover, the $NiFe_2O_4$@SNF possessed a robust saturation magnetization (M_s) of 13.7 emu g^{-1}. Taken into consideration of the relative amount of $NiFe_2O_4$ NPs in membranes (31.6 wt%), an promising equivalent M_s of 43.4 emu g^{-1} could be analogized to the synthesized $NiFe_2O_4$ NPs, which was comparable to the theoretical M_s of 50 emu g^{-1} calculated using Neel's sublattice theory and to the reported value of 56 emu g^{-1} for the bulk sample.[22]

In dramatic contrast to the brittle nature of ceramic nanofibrous membranes, the $NiFe_2O_4$@SNF can bear a repeated bending through 180° with no apparent damage, and can recover their original shape after the release of the stress, as shown in Fig. S2 and Movie S1. The tensile stress-strain curves presented in Fig. S3 revealed that the $NiFe_2O_4$@SNF exhibited a robust strength of 3.1 MPa, which were obvious higher than that of the commercial nonwoven mats.[11] In comparison, although some ceramic magnetic membranes have been constructed, but their brittleness renders them impractical for most applications.[6, 19] This unexpected flexibility was owing to the high aspect ratio (>1000) and entanglement of silica nanofibers, which could absorb the tensile stress at a high level by the bending and slipping of individual silica nanofibers.[2,11] More interestingly, Fig. 4a demonstrated that a small magnet can induce reversible and large bending deformation of the $NiFe_2O_4$@SNF (see also Movie S2). Previous studies have reported that magnetic nanoparticle-containing liquid ferrogels and hydrogels had similar responsiveness, however, drying of such gels typically results in brittle materials.[4,7] The above results suggest that this dry flexible membrane actuators may be used in conditions similar to soft electronic devices.

We further demonstrated that, the $NiFe_2O_4$@SNF whic combined the enhanced mesoporous structure and magnet property can be used for efficient adsorption of organi containments in water. A typical organic containment– methylene blue (MB) dye was used as an example to test th adsorption performance of $NiFe_2O_4$@SNF. As shown in Figs. 4 and S4, the $NiFe_2O_4$@SNF could adsorb 85% of MB for 15 mi and achieve completely adsorption of MB for 25 mi Significantly, after adsorption, the $NiFe_2O_4$@SNF could be facilely separated by an external magnet without tedi recycling process, which is of great importance for real applications.

Another unique feature of the $NiFe_2O_4$@SNF was their robu selective wettability. The $NiFe_2O_4$@SNF was full of high surfac energy hydroxyl groups on its surface, leading to superamphiphilicity in air with both the water contact angle an oil contact angle (OCA) of 0°.[23] Meanwhile, the oleophobicit appeared immediately for $NiFe_2O_4$@SNF after being immerse in water, with a robust underwater OCA of 145°, as shown in Fig 4c. Thus, the $NiFe_2O_4$@SNF exhibited low adhesion to an o droplet with no permeation, whereas a water droplet can rapidly permeate through the membranes. Moreover, he unique hierarchical porous structure provided numer microporous channels for the water transportation; thus effective separation of oil/water emulsions by th $NiFe_2O_4$@SNF was expected. A surfactant-stabilized (Tween 8 oil (petroleum ether was taken as an example)-in-water microemulsions with an average droplet size of 4.52 μm wa prepared (Fig. S5) to test the separation performance. Fig. 4d showed the solely gravity-driven separation of surfactan stabilized emulsions using the $NiFe_2O_4$@SNF; the water

Chemcomm Accepted Manuscript

immediately permeated through the membranes, whereas the emulsified oil droplets were retained above (Movie S3). The optical microscopic images of collected filtrate showed that no droplet was observed in the collected filtrate in the whole image, indicating the high effectiveness for separating microemulsions. The $NiFe_2O_4$@SNF exhibited a high separation flux of 1580 ± 106 L m^{-2} h^{-1}, which was obviously higher than that of other pressure-driven separation materials. Considering that the separation was driven solely by gravity, such separation performance is very promising from the viewpoint of energy conservation, in contrast to the traditional filtration membranes such as UF membranes where an applied pressure of more than 10^5 Pa is usually used to accomplish emulsion separation.[11,23]

In summary, we have demonstrated a general strategy for the scalable fabrication of magnetic, flexible, and hierarchical porous $NiFe_2O_4$@SNF by combining gelatin dip-coating with electrospun nanofibers. The introduction of gelatin carrier enables the non-agglomerated growth of $NiFe_2O_4$ NPs with diameter of 20-50 nm on silica nanofiber surface, and achieving uniform distribution and high concentration. With their magnetic property, flexibility, selective wettability, mesoporousity, and unique multifunctionality in terms of magnetic responsiveness, dyes adsorption, and emulsion separation, we envision that such exceptional $NiFe_2O_4$@SNF will open up numerous opportunities for a range of applications in soft electronic devices, drug delivery, medical diagnosis, ferrofluids, liquid separation, magnetic resonance imaging, and magnetic adsorption. The successful synthesis of such materials may also provide new insights into design and development of other functional membranes for various applications.

This work is supported by the National Natural Science Foundation of China (No. U1232116 and 51322304), the Fundamental Research Funds for the Central Universities, and the “DHU Distinguished Young Professor Program”.

Notes and references

1 S. C. Warren, M. R. Perkins, A. M. Adams, M. Kamperman, A. A. Burns, H. Arora, E. Herz, T. Suteewong, H. Sai, Z. H. Li, J. Werner, J. H. Song, U. Werner-Zwanziger, J. W. Zwanziger, M. Gratzel, F. J. DiSalvo and U. Wiesner, *Nat. Mater.*, 2012, **11**, 460-467.
2 J. Cai, S. Liu, J. Feng, S. Kimura, M. Wada, S. Kuga and L. Zhang, *Angew. Chem. Int. Ed.*, 2012, **51**, 2076-2079.
3 M. Hessien, P. Léone, M. Suchaud, B. LeBeau, H. Nouali, Y. Guari and E. Prouzet, *Chem. Commun.*, 2012, **48**, 10022-10024.
4 M. K. K. Oo, Y. M. Yang, Y. Hu, M. Gomez, H. Du and H. J. Wang, *ACS Nano*, 2012, **6**, 1939-1947.
5 B. Y. Li, B. B. Jiang, D. J. Fauth, M. L. Gray, H. W. Pennline and G. A. Richards, *Chem. Commun.*, 2011, **47**, 1719-1721.
6 N. A. M. Barakat, K. A. Khalil, I. H. Mahmoud, M. A. Kanjwal, F. A. Sheikh and H. Y. Kim, *J. Phys. Chem. C*, 2010, **114**, 15589-15593.
7 Y. P. Li, W. W. Xiao, K. Xiao, L. Berti, J. T. Luo, H. P. Tseng, G. Fung and K. S. Lam, *Angew. Chem. Int. Ed.*, 2012, **51**, 2864-2869.
8 Y. E. Miao, R. Y. Wang, D. Chen, Z. Y. Liu and T. X. Liu, *ACS Appl. Mater. Interfaces*, 2012, **4**, 5353-5359.
9 J. J. Yuan, P. X. Zhu, N. Fukazawa and R. H. Jin, *Adv. Funct. Mater.*, 2006, **16**, 2205-2212.
10 X. Deng, L. Mammen, Y. Zhao, P. Lellig, K. Müllen, C. Li, H. J. Butt and D. Vollmer, *Adv. Mater.*, 2011, **23**, 2962-2965.
11 Y. Si, J. Y. Yu, X. M. Tang, J. L. Ge and B. Ding, *Nat. Commun.*, 2014, **5**, 9.
12 12.X. Wang, B. Ding, G. Sun, M. Wang and J. Yu, *Prog. Mater. Sci.*, 2013, **58**, 1173-1243.
13 S. Sinha-Ray, M. W. Lee, S. Sinha-Ray, S. An, B. Pourdeyhimi, S. S. Yoon and A. L. Yarin, *J. Mater. Chem. C*, 2013, **1**, 3491.
14 J. Sundaram, T. D. Durance and R. Wang, *Acta Biomater.*, 2008, **4**, 932-942.
15 P. R. Sarika, P. R. Anil Kumar, D. K. Raj and N. R. James, *Carbohydr. Polym.*, 2015, **119**, 118-125.
16 M. A. Gabal, R. S. Al-luhaibi and Y. M. Al Angari, *J. Hazard. Mater.*, 2013, **246-247**, 227-233.
17 I. Baroudi, C. Simonnet-Jégat, C. Roch-Marchal, N. Leclerc-Laronze, C. Livage, C. Martineau, C. Gervais, E. Cadot, F. Carr B. Fayolle and N. Steunou, *Chem. Mater.*, 2015, **27**, 1452-1464.
18 S. Maensiri, C. Masingboon, B. Boonchom and S. Seraphin, *Scripta Mater.*, 2007, **56**, 797-800.
19 Y. Si, T. Ren, B. Ding, J. Yu and G. Sun, *J. Mater. Chem.*, 20__, **22**, 4619-4622.
20 L. P. Li, G. S. Li, R. L. Smith and H. Inomata, *Chem. Mater.*, 2000, **12**, 3705-3714.
21 Y. Si, T. Ren, Y. Li, B. Ding and J. Yu, *Carbon*, 2012, **50**, 5176-5185.
22 V. Sepelak, K. Tkacova, V. V. Boldyrev, S. Wimann and K. D. Becker, *Physica B*, 1997, **234–236**, 617-619.
23 Y. Si, Q. Fu, X. Wang, J. Zhu, J. Yu, G. Sun and B. Ding, *ACS Nano*, 2015, **9**, 3791-3799.

ChemComm Accepted Manuscript

This journal is © The Royal Society of Chemistry 20xx